

Diode parameters extraction and study of space charge limited current in (Ag, Au)/CoS₂ Schottky diodes

S.M.T. Kazmi^a, Z. Zahoor^b, N.T. Yusra^b, M.H. Bhatti^a, M.F. Afsar^a, F. Sher^c, Haroon-ur Rashid^b, M.A. Rafiq^{a,*}

^a Condensed Matter Physics Laboratories, Department of Physics and Applied Mathematics, Pakistan Institute of Engineering and Applied Sciences (PIEAS), P. O. Nilore, Islamabad, 4650, Pakistan

^b Department of Electrical Engineering, Pakistan Institute of Engineering and Applied Sciences (PIEAS), P. O. Nilore, Islamabad, 4650, Pakistan

^c Department of Chemistry, SBA School of Science and Engineering, LUMS, Lahore, Pakistan

ARTICLE INFO

Keywords:

Cobalt sulfide
Schottky diode
Space charge limited current
Richardson's coefficient
Electron transport
Solid state reaction

ABSTRACT

We investigated the electron transport properties of cobalt sulphide Schottky diodes with Au and Ag metal contacts. Pure CoS₂ nanoplates were synthesized using solid state reaction method. From temperature dependent IV characteristics diode parameters including ideality factor, barrier height and Richardson coefficient were calculated for Au/CoS₂ and Ag/CoS₂ diodes. The value of barrier height increased with increasing temperature for both devices, however Ideality factor showed different trend. The values of modified Richardson coefficient by assuming the Gaussian distribution of the barrier heights turns out to be $244.20 \text{ Acm}^{-2}\text{K}^{-2}$ and $348.20 \text{ Acm}^{-2}\text{K}^{-2}$ for Au/CoS₂ and Ag/CoS₂ diodes respectively. At high voltages we observed Space Charge Limited Current (SCLC) with an exponential trap distribution in Au/CoS₂ diode. The density of the traps and characteristic temperature associated with these traps were determined to be $2.47 \times 10^{14} \text{ cm}^{-3}$ and 141 K, respectively.

1. Introduction

Cobalt sulfide is an important semiconductor material and its stoichiometric complexity leads to a number of phases like CoS, CoS₂, Co₃S₄, etc. With its distinctive electrical, magnetic, and catalytic properties cobalt sulfide is a promising candidate in various applications, including supercapacitors [1,2], solar selective coatings [3], catalysis for hydrogen generation [4,5], and field effect transistors [6,7]. In the potential applications of cobalt sulfide in various devices, a comprehensive understanding of its electrical properties and transport mechanism are important. Especially in semiconductor devices metal-semiconductor (MS) contact named as Schottky diode is important aspect. Today, the Schottky diodes are used as microwave diodes, rectifiers, UV detectors, photo sensors, switching diodes and solar cells [8–12]. Due to the technological importance of Schottky diodes, investigation of diode parameters such as Richardson coefficient, ideality factor, potential barrier height, and a full understanding of carrier's conduction mechanisms is of great importance.

The Schottky diode parameters can be extracted from the

investigation of the current-voltage (IV) characteristics, based on thermionic emission diffusion (TE) theory [13]. Only study of IV characteristics at room temperature does not provide enough information regarding the current conduction mechanisms and barriers at the metal semiconductor interface. Temperature-dependent IV measurements provide considerable information regarding diode parameters and current conduction mechanisms [14,15]. Since the Richardson constant is used to calculate the barrier height, it is necessary to know its precise value or its value in temperature range in which barrier height is being calculated. However, the large disparity between the expected and estimated Richardson coefficient using classical TE model could be due to potential fluctuations and lateral inhomogeneity of the barrier at an interface. More accurate value of Richardson coefficients can be calculated by assuming the Gaussian distribution of the potential barrier heights [13,16,17]. Different current conduction mechanisms can be distinguished on the bases of power law ($I \sim V^m$). The lnI-InV plot can have different regions with different slopes (m), these regions correspond to different current conduction mechanisms [18,19]. A region with slope ~ 1 , especially at low voltages corresponds to ohmic region.

* Corresponding author.

E-mail address: aftab@cantab.net (M.A. Rafiq).

Because it follows Ohm's law as long as the intrinsic electron concentration is larger than the injected electron concentration. Space charge effects become important with the increasing voltage when the intrinsic electron concentration is comparable with the injected electrons. At higher voltages, larger charge injection leads to the space charge limited current (SCLC). SCLC region with slope ~ 2 verifies that charge limited conduction is dominated by an exponential distribution of traps.

In this paper we have studied the diode parameters and conduction mechanism of CoS_2 with silver and gold contact based Schottky diodes. Richardson coefficient was extracted from the modified Richardson plot by assuming the Gaussian distribution of the barrier heights. From temperature dependent IV characteristics SCLC conduction mechanism was only observed in Au/ CoS_2 based Schottky diode in specific voltage range. The characteristic energy of the trap distribution and traps density was calculated from crossover voltage.

2. Experimental details

The CoS_2 was prepared by solid state reaction method at ambient pressure in inert environment using Cobalt Nitrate and Thiourea were used as precursors. The precursors were of analytical grade and used without further purification. Firstly, cobalt nitrate and thiourea were mixed in the ratio 1:2. The resulting mixture was fine grounded using mortar and pestle for 40 min. The ground powder was heated in a tube furnace at 500 °C for 2 h under argon flow. This resulted in the

formation of CoS_2 .

Fig. 1 (a) shows the X-ray Diffraction (XRD) pattern of CoS_2 nanoplates. The XRD pattern was acquired using $\text{Cu K}\alpha$ radiation ($\lambda = 1.54 \text{ \AA}$). The XRD pattern was matched with the JCPDS card number 00-041-1471 indicating that the synthesized CoS_2 nanoplates are pure. The XRD pattern also reveals that the synthesized CoS_2 nanoplates have cubic phase with space group Pa3. The lattice parameter ' a ' is 5.54 \AA . The crystallite size CoS_2 nanoplates was calculated using the Debye-Scherrer's Equation:

$$D = \frac{K\lambda}{\beta \cos \theta} \quad (1)$$

The crystallite size of CoS_2 nanoplates was found to be 20.85 nm. Moreover, lattice strain in CoS_2 nanoplates was determined from the XRD pattern using the Stokes-Wilson equation:

$$\epsilon = \frac{\beta}{4 \tan \theta} \quad (2)$$

The average lattice strain in CoS_2 nanoplates was 0.49.

Fig. 1 (b) shows the scanning electron micrograph (SEM) of CoS_2 nanoplates. Clear nanoplates morphology can be seen with lateral sizes of CoS_2 nanoplates ranging from few nm to few micrometers. The energy dispersive spectrum (EDS) shown in **Fig. 1** (c) indicates the presence of Cobalt and Sulfur in the sample indicating that pure CoS_2 nanoplates have been formed. **Fig. 1** (d) shows the high-resolution transmission

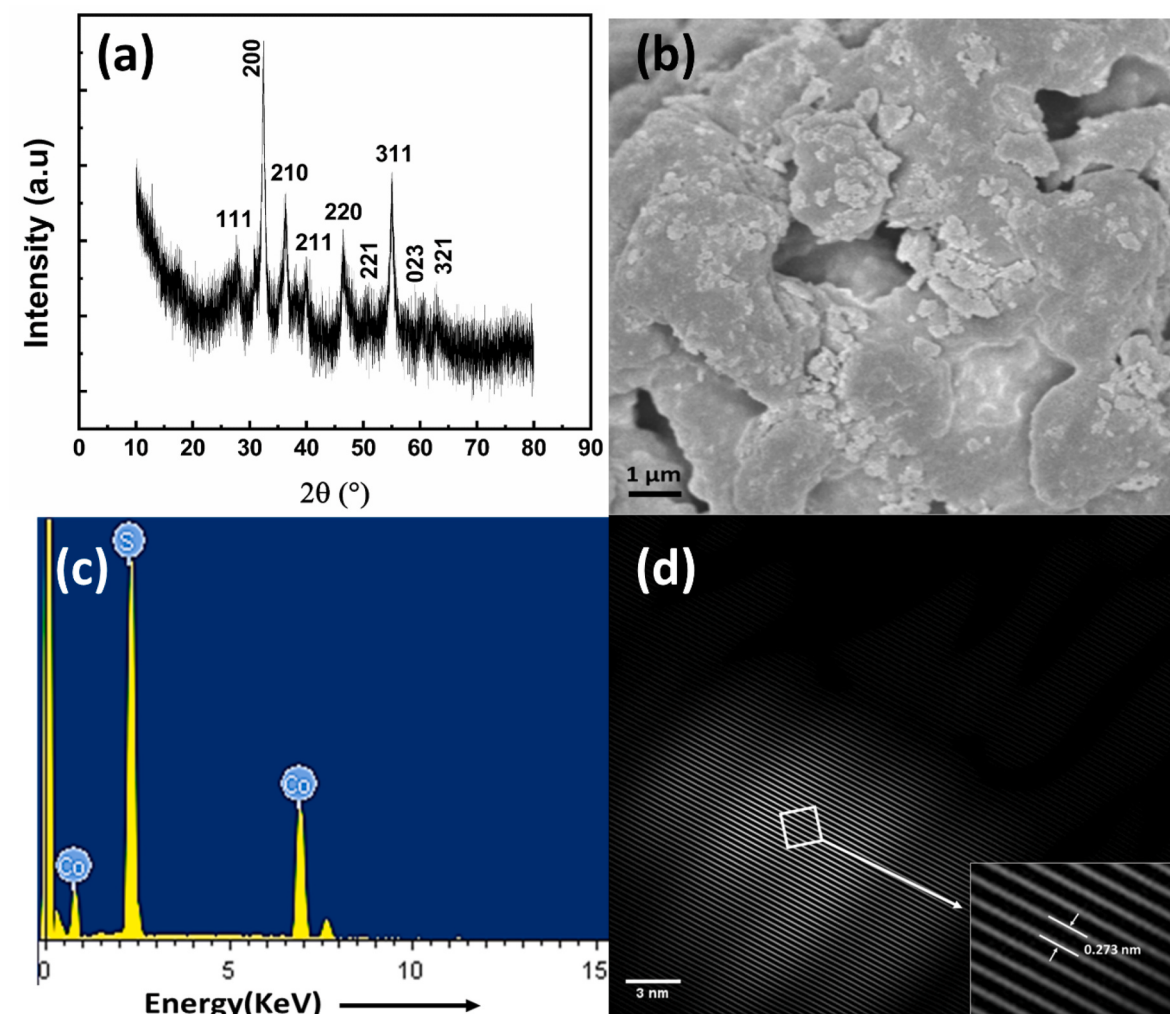


Fig. 1. (a) XRD spectrum of CoS_2 (b) SEM micrograph of synthesized CoS_2 nanoplates (c) EDS spectrum of CoS_2 showing the presence of Co and S only (d) TEM image of CoS_2 confirming the d-spacing to be 0.273 nm which is consistent with XRD analysis.

electron microscope (TEM) image of CoS_2 nanoplates. Clear crystalline structure is visible in the micrograph [20]. The d-spacing calculated from the image turned out to be 2.73 Å and matches with that obtained from XRD analysis.

To fabricate CoS_2 nanoplates diode, Si wafer with a layer of native $\text{SiO}_2 \sim 10\text{--}20$ nm was used as substrates. The wafers were cleaned in acetone, ethanol and DI water for 5 min in ultrasonic bath followed by nitrogen blow to dry the wafer. The pure silver and gold contacts were deposited on cleaned wafer by sputtering using shadow mask. To prepare a suspension, 0.1 g of CoS_2 was added in 10 ml of IPA (Isopropyl Alcohol) in the ultrasonic bath for 30 min at room temperature. The resulting suspension was deposited with a blunt needle on the substrates between the metal contacts. Depending upon the work function of metal (Φ_m) and semiconductor (Φ_s) the rectifying (Schottky) or ohmic contact forms. In the case of metal and an n-type semiconductor, a Schottky contact is formed when $\Phi_m > \Phi_s$, and an Ohmic contact is formed when $\Phi_m < \Phi_s$.

3. Results and discussion

Temperature dependent IV characteristics of CoS_2 nanoplates with gold and silver contacts were performed using Agilent 4156C semiconductor parameter analyzer from 300 K to 120 K. Fig. 2 (a & b) shows the IV characteristics of Au/ CoS_2 nanoplates and Ag/ CoS_2 nanoplates in temperature range 300–120 K and 300–185 K respectively. Both IV characteristics exhibit symmetric, temperature dependent and nonlinear semiconducting behaviour. Nonlinear behaviour is more prominent in Au/ CoS_2 however current in Ag/ CoS_2 diode is higher than that in the Au/ CoS_2 diode. At 300 K and 0.35 V, the current values are 0.70 μA and 0.97 mA for Ag/ CoS_2 and Au/ CoS_2 device respectively. Ag/ CoS_2 device shows ~ 1900 times greater current at 186 K and ~ 1400 times greater at 300 K.

For device applications the understanding of the carrier's transport properties of the CoS_2 based Schottky diodes is very important. The thermionic emission model suggests the forward biased current in Schottky barrier diode as:

$$I = I_s \left[\exp\left(\frac{qV}{nkT}\right) - 1 \right] \quad (3)$$

where V is the applied voltage, n is the ideality factor, q is the charge of electron, k is the Boltzmann constant, and saturation current is represented by I_s :

$$I_s = AA^* T^2 \exp\left(-\frac{q\varphi_b}{kT}\right) \quad (4)$$

here A is the effective diode area, A^* is the Richardson constant and φ_b is the Schottky barrier height of diode [21]. The barrier height is expressed as

$$\varphi_b = \frac{kT}{q} \ln\left(\frac{AA^* T^2}{I_s}\right) \quad (5)$$

Equation (3) was fitted to the IV characteristics of both diodes as shown in Fig. 3 (a & b). It can be seen from Fig. 3 (a & b) that equation (3) fits well to the experimental data of both diodes. From the fitting, saturation current and ideality factor of both devices were extracted at different temperatures.

The extracted barrier height and ideality factor of Au/ CoS_2 and Ag/ CoS_2 diodes at different temperatures are as shown in Fig. 4 (a & b) respectively. Au/ CoS_2 has larger barrier height and smaller ideality factor than those of Ag/ CoS_2 at specific temperature. The lower value of the barrier height for Ag/ CoS_2 diode explains the higher current in it as compared to that of Au/ CoS_2 diode. For Au/ CoS_2 , φ_b value increased and n decreased with the increasing temperature (shown in Fig. 3(a)). The increase in φ_b with an increase in temperature may be due to the reason that the inhomogeneity between metal (Au, Ag) and CoS_2 interface is enhanced with rise in temperature [22]. The decrease in n with an increase in temperature is attributed to relative increase of recombination in the bulk of the CoS_2 nanoplates as compared to the recombination in the space-charge region [23]. For Ag/ CoS_2 n increased with the increasing temperature (shown in Fig. 3(b)). Similar behaviour of n with temperatures has been observed in monocrystalline silicon solar cells [24,25].

The Richardson coefficient can be determined experimentally from conventional Richardson plot by rewriting equation (2) as

$$\ln\left(\frac{I_s}{T^2}\right) = \ln(AA^*) - \frac{q\varphi_b}{kT} \quad (6)$$

The equation shows that the y-intercept of $\ln(I_s/T^2)$ vs $1/T$ curve (not shown) yields Richardson coefficient. The values of Richardson coefficient turn out to be $8.48 \times 10^{-8} \text{ Acm}^{-2}\text{K}^{-2}$ and $4.63 \times 10^{-4} \text{ Acm}^{-2}\text{K}^{-2}$ for Au/ CoS_2 and Ag/ CoS_2 respectively. However the calculated values of Richardson constant are smaller than its expected value. The huge difference in Richardson constant values can be due to the barrier's lateral inhomogeneity and potential fluctuations at an interface [17].

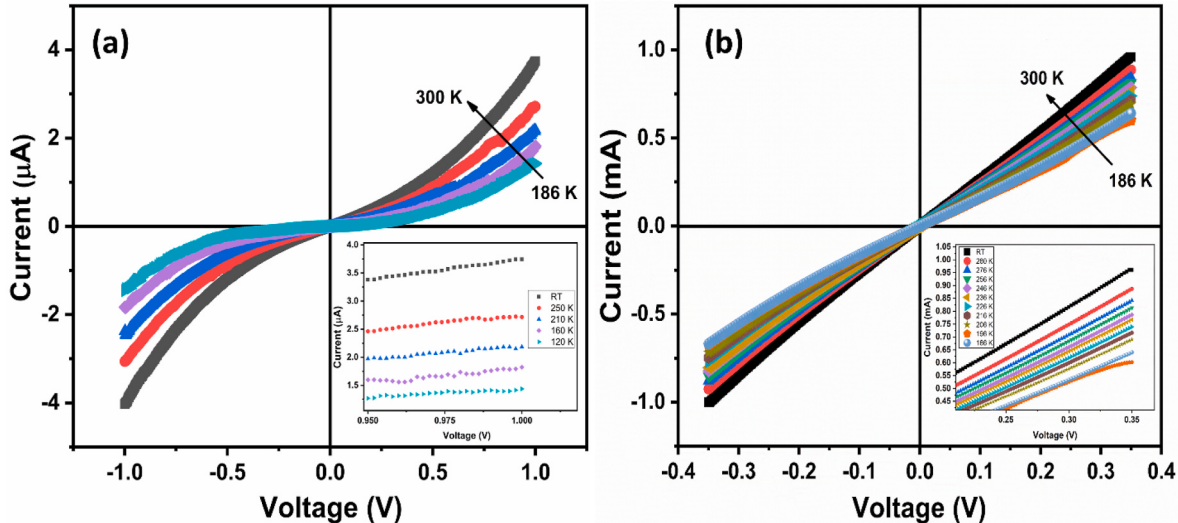


Fig. 2. Current vs voltage characteristics of (a) Au/ CoS_2 in temperature range 120 K–300 K and (b) Ag/ CoS_2 in temperature range 186 K–300 K.

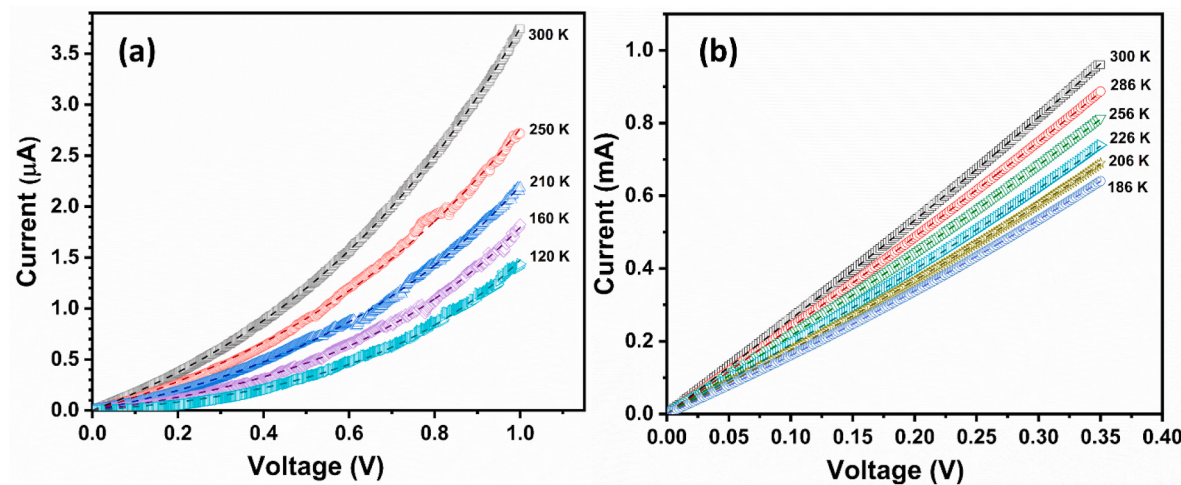


Fig. 3. Fitting of thermionic emission model on forward bias IV characteristics of (a) Au/CoS₂ and (b) Ag/CoS₂ schottky diodes at different temperatures.

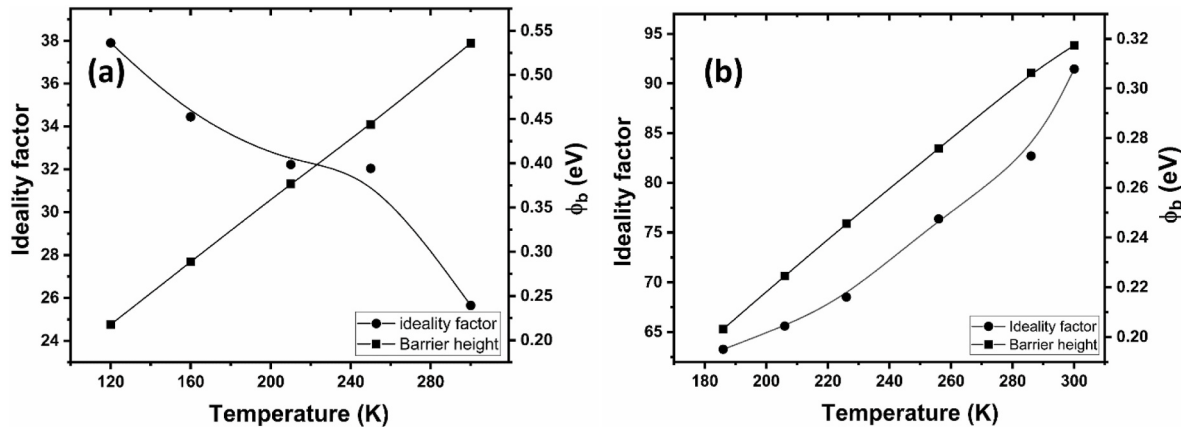


Fig. 4. Temperature dependence of Ideality factor(n) and barrier height (ϕ_b) of (a) Au/CoS₂ and (b) Ag/CoS₂ schottky diodes.

These observed inhomogeneities can be explained by assuming the Gaussian distribution of the barrier heights with a mean value ϕ_{b0} and standard deviation σ given by

$$\phi_b = \phi_{b0} - \frac{q\sigma^2}{2kT} \quad (7)$$

ϕ_b is the experimentally measured apparent barrier height. The standard deviation σ of the gaussian can be calculated from slope of ϕ_b vs $1/T$ plot [26]. The value of σ was measured to be 98 mV and 105 mV for Ag/CoS₂ and Au/CoS₂ respectively. This extracted σ can be used to calculate the Richardson constant from the gaussian corrected Richardson plots using:

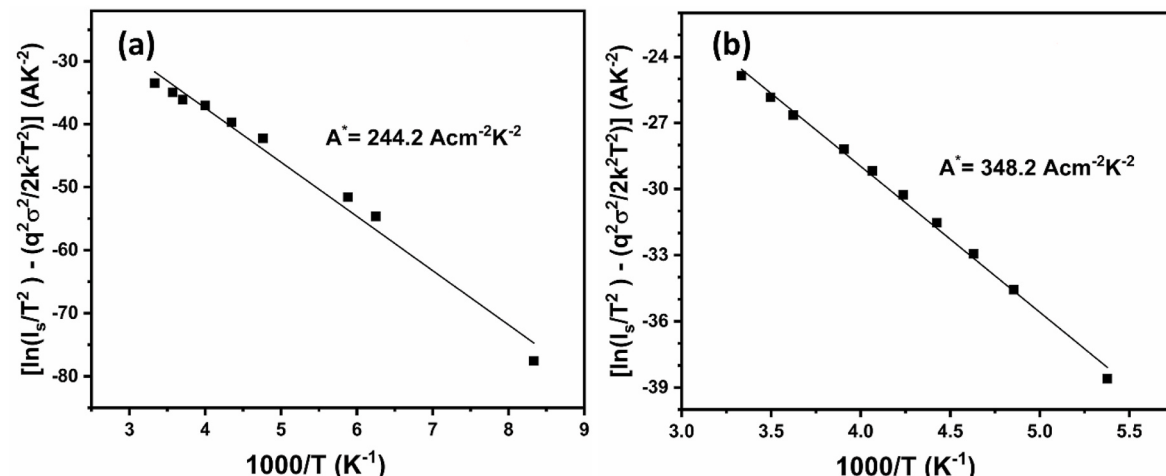


Fig. 5. Modified Richardson plots according to Gaussian distribution of the barrier heights for (a) Au/CoS₂ and (b) Ag/CoS₂.

$$\ln\left(\frac{I_s}{T^2}\right) - \left(\frac{q^2\sigma^2}{2k^2T^2}\right) = \ln(AA^*) - \frac{q\varphi_b}{kT} \quad (8)$$

The modified $\ln\left(\frac{I_s}{T^2}\right) - \left(\frac{q^2\sigma^2}{2k^2T^2}\right)$ vs $1/T$ plot gives the straight line with intercept related to A^* and slope directly gives the mean barrier height as shown in Fig. 5 (a & b). The value of modified Richardson coefficient turns out to be $244.20 \text{ Acm}^{-2}\text{K}^{-2}$ and $348.20 \text{ Acm}^{-2}\text{K}^{-2}$ for Au/CoS₂ and Ag/CoS₂ respectively. From this fitting the obtained mean barrier height is 0.74 eV and 0.57 eV for Au/CoS₂ and Ag/CoS₂ respectively. Therefore we conclude that the assumption of Gaussian distribution of the barrier heights yields acceptable values of Richardson coefficient.

To further investigate the transport mechanism of both devices, double logarithmic $\ln(I)$ - $\ln(V)$ graphs are plotted as the current conduction mechanisms are distinguish on the basis of power law ($I \propto V^m$). The $\ln I$ - $\ln V$ plot of Au/CoS₂ device is shown in Fig. 6 (a). This figure shows two distinct regions, the first region at low voltages is the ohmic region with slope of ~ 1 that obey ohm's law and at high voltages second region correspond to the space charge limited current (SCLC) with exponential distribution of traps [27]. SCLC occurs, when density of injected free carriers at contact is larger as compare to the internal carrier concentration. In SCLC region the values of slopes are ~ 1.9 - 2.3 at 180-120 K respectively. The slope increases with decreasing temperature indicates that trapped electrons are more stable. In case of SCLC with exponential distribution of traps, the current density is given by:

$$J = q^{1-l} \mu N_{DOS} \left(\frac{2l+1}{l+1} \right)^{l+1} \left(\frac{l}{l+1} \frac{\varepsilon_s \varepsilon_o}{N_t} \right)^l V^{l+1} \quad (9)$$

here, μ is the carrier mobility, q is the charge of electron, N_{DOS} is the density of states in the relevant band, N_t is the density of traps, d is the thickness of sample, ε_s is the dielectric constant of material, l is the parameter given by $l = \frac{T_c}{T}$ and T_c is the characteristic temperature that characterizes an exponential distribution of trap density. This equation gives power law dependence ($I \propto V^m$) with $m = l + 1$. From the slope of m vs $1/T$ plot T_c turn out to be 141 K as show in inset to Fig. 6 (b). The characteristic energy of traps distribution can be calculated from $E_c = k_b T_c$ that is 12 meV for this device. As shown in figure, extrapolations of $\ln(I)$ - $\ln(V)$ plot meet at single point called "cross over voltage (V_c)" which can be written as

$$V_c = \frac{qN_t d^2}{2\varepsilon_s \varepsilon_o} \quad (10)$$

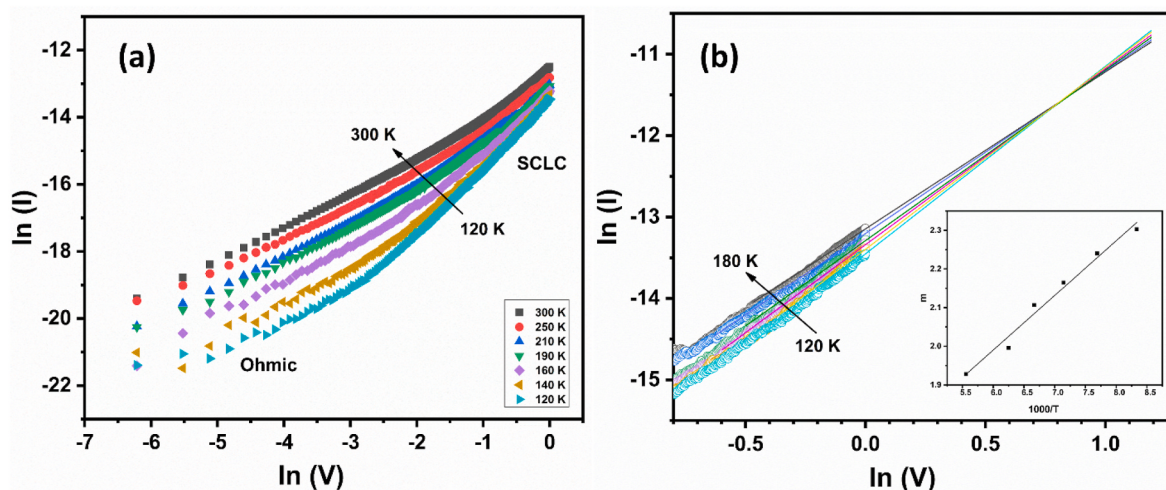


Fig. 6. (a) $\ln I$ vs $\ln V$ graph of Au/CoS₂ diode in 120 K-300 K temperature range to explain the conduction mechanisms. The first region at low voltages with slope ~ 1 is the ohmic region and the second region corresponds to SCLC. (b) Power law fitting on SCLC region for 120 K-180 K temperature range. The intercept of the linear fits gives cross over voltage $V_c = 2.23$ V. The inset shows the slopes of these fits as function of inverse temperature.

As from the figure V_c for Au/CoS₂ is 2.23 V. The value of ε_s is calculated from the complex impedance spectroscopy [28]. The value of ε_s decreases with increasing frequency and at higher frequencies reached an almost constant value at all temperatures [29]. This constant value of dielectric constant of CoS₂ at higher frequencies evaluated to be $\varepsilon_s \sim 144$. By substituting this value of V_c and ε_s in equation, the trap density turns out to be $N_t = 2.47 \times 10^{14} \text{ cm}^{-3}$.

4. Conclusion

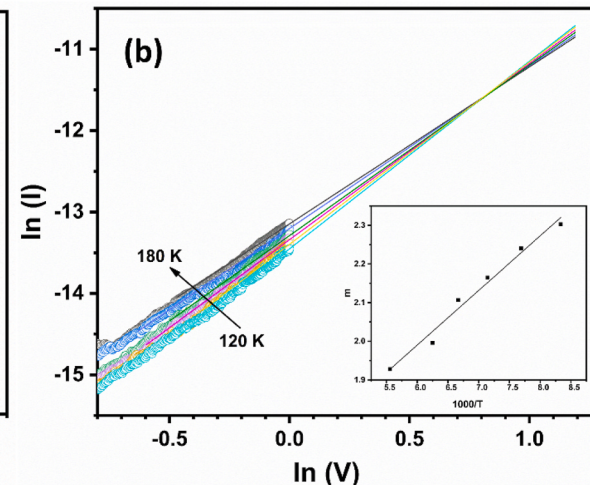
CoS₂ nanoplates were synthesized using solid state reaction method at 500 °C in inert environment. XRD, SEM, EDS and TEM analysis confirmed the formation of pure CoS₂ nanoplates. We investigated the electron transport properties of CoS₂ nanoplates Schottky diodes with Au and Ag metal contacts. From temperature dependent IV characteristics, diode parameters like ideality factor, barrier height and Richardson coefficient were calculated for both devices. The value of barrier height increased with increasing temperature for both devices. However n increased for Ag/CoS₂ and decreased for Ag/CoS₂ with increasing temperature. The values of Apparent Richardson coefficient turn out to be $8.48 \times 10^{-8} \text{ Acm}^{-2}\text{K}^{-2}$ and $4.63 \times 10^{-4} \text{ Acm}^{-2}\text{K}^{-2}$ for Au/CoS₂ and Ag/CoS₂ respectively. However the values of modified Richardson coefficient by assuming the Gaussian distribution of the barrier heights were $244.20 \text{ Acm}^{-2}\text{K}^{-2}$ and $348.20 \text{ Acm}^{-2}\text{K}^{-2}$ for Au/CoS₂ and Ag/CoS₂ respectively. At low voltages we observed Ohmic behaviour followed by SCLC at higher voltages with an exponential trap distribution in Au/CoS₂. The density of the traps and characteristic temperature associated with these traps were determined to be $2.47 \times 10^{14} \text{ cm}^{-3}$ and 141 K, respectively.

Credit author statement

Conceptualization: M. A. Rafiq. Formal analysis: S.M.T. Kazmi Z. Zahoor, N.T. Yusra. Data Curation: S.M.T. Kazmi Z. Zahoor, N.T. Yusra, Investigation: S.M.T. Kazmi, M.H Bhatti, M. A. Rafiq. Writing - original draft: S.M.T. Kazmi Z. Zahoor, N.T. Yusra. Writing - review & editing: M. A. Rafiq, F Sher. Supervision: M.A. Rafiq, Haroon-ur-Rashid. Resources: F Sher, M. F. Afasr, M.H Bhatti, M. A. Rafiq.

Declaration of competing interest

The authors declare that they have no known competing financial interests or personal relationships that could have appeared to influence



the work reported in this paper.

Data availability

Data will be made available on request.

References

- [1] C.K. Ranaweera, Z. Wang, E. Alqurashi, P.K. Kahol, P.R. Dvornic, B.K. Gupta, K. Ramasamy, A.D. Mohite, G. Gupta, R.K. Gupta, Highly stable hollow bifunctional cobalt sulfides for flexible supercapacitors and hydrogen evolution, *J. Mater. Chem. A* 4 (2016) 9014–9018.
- [2] L.G. Beka, X. Li, X. Wang, C. Han, W. Liu, Reduced graphene oxide/CoS₂ porous nanoparticle hybrid electrode material for supercapacitor application, *RSC Adv.* 9 (2019) 26637–26645.
- [3] J. Nezamifar, K. Ghani, N. Kiomarsipour, Solvothermal synthesis of cobalt and copper sulfides nanoparticles with high light absorptance for new solar selective coatings, *J. Nanostruct.* 5 (2015) 203–207.
- [4] Y. Sun, C. Liu, D.C. Grauer, J. Yano, J.R. Long, P. Yang, C.J. Chang, Electrodeposited cobalt-sulfide catalyst for electrochemical and photoelectrochemical hydrogen generation from water, *J. Am. Chem. Soc.* 135 (2013) 17699–17702.
- [5] X. Chen, Y. Yu, J. Li, P. Deng, C. Wang, Y. Hua, Y. Shen, X. Tian, Recent advances in cobalt disulfide for electrochemical hydrogen evolution reaction, *Int. J. Hydrogen Energy* 48 (2023) 9231–9243.
- [6] R. Mathew, J. Ajayan, Material processing, performance and reliability of MoS₂ field effect transistor (FET) technology- A critical review, *Mater. Sci. Semicond. Process.* 160 (2023), 107397.
- [7] B. Mereu, G. Sarau, E. Pentia, V. Draghici, M. Lisca, T. Botila, L. Pintilie, Field-effect transistor based on nanometric thin CdS films, *Mater. Sci. Eng., B* 109 (2004) 260–263.
- [8] B. Ezhilmalaran, A. Patra, S. Benny, S.M. R, A.V. V, S.V. Bhat, C.S. Rout, Recent developments in the photodetector applications of Schottky diodes based on 2D materials, *J. Mater. Chem. C* 9 (2021) 6122–6150.
- [9] N.A. Al-Ahmadi, Metal oxide semiconductor-based Schottky diodes: a review of recent advances, *Mater. Res. Express* 7 (2020), 032001.
- [10] I. Missoum, Y.S. Ocak, M. Benhalilba, C.E. Benouis, A. Chaker, Microelectronic properties of organic Schottky diodes based on MgPc for solar cell applications, *Synth. Met.* 214 (2016) 76–81.
- [11] I. Capan, 4H-SiC Schottky barrier diodes as radiation detectors: a review, *Electronics* 11 (2022) 532.
- [12] A.K.U. Shubham Tayal, Deepak Kumar, Shiromani Balmukund Rahi, Emerging Low-Power Semiconductor Devices: Applications for Future Technology Nodes, first ed., 2022.
- [13] S. Chand, J. Kumar, Current-voltage characteristics and barrier parameters of Pd2Si/p-Si(111) Schottky diodes in a wide temperature range, *Semicond. Sci. Technol.* 10 (1995) 1680.
- [14] Z. Imran, M.A. Rafiq, M.M. Hasan, Charge carrier transport mechanisms in perovskite CdTiO₃ fibers, *AIP Adv.* 4 (2014).
- [15] A. Büyükbaba Uluşan, A. Tataroğlu, Y. Azizian-Kalandaragh, Ş. Altindal, On the conduction mechanisms of Au/(Cu₂O–CuO–PVA)/n-Si (MPS) Schottky barrier diodes (SBDs) using current–voltage–temperature (I–V–T) characteristics, *J. Mater. Sci. Mater. Electron.* 29 (2018) 159–170.
- [16] M.A. Mayimele, M. Dialet, W. Mtangi, F.D. Auret, Temperature-dependent current–voltage characteristics of Pd/ZnO Schottky barrier diodes and the determination of the Richardson constant, *Mater. Sci. Semicond. Process.* 34 (2015) 359–364.
- [17] C.P.Y. Wong, C. Troadec, A.T.S. Wee, K.E.J. Goh, Gaussian thermionic emission model for analysis Au/MoS₂ Schottky-barrier devices, *Phys. Rev. Appl.* 14 (2020), 054027.
- [18] M.A. Lampert, Volume-controlled current injection in insulators, *Rep. Prog. Phys.* 27 (1964) 329.
- [19] M. Ahmad, K. Rasool, M.A. Rafiq, M.M. Hasan, C.B. Li, Z.A.K. Durrani, Effect of incorporation of zinc sulfide nanoparticles on carrier transport in silicon nanowires, *Phys. E Low-dimens. Syst. Nanostruct.* 45 (2012) 201–206.
- [20] N. Kumar, N. Raman, A. Sundaresan, Synthesis and properties of cobalt sulfide phases: CoS₂ and Co₉S₈, *Z. Anorg. Allg. Chem.* 640 (2014) 1069–1074.
- [21] M. Shah, M.H. Sayyad, K.S. Karimov, F. Wahab, Electrical characterization of the ITO/NiPc/PEDOT : PSS junction diode, *J. Phys. Appl. Phys.* 43 (2010), 405104.
- [22] L. Singh, The temperature dependent electrical characteristics of Au/(n)PbS Schottky barrier junction fabricated by chemical bath deposition method, *J. Ovonics Res.* 15 (2019) 15–26.
- [23] A. Rao, S. Krishnan, G. Sajeev, K. Siddappa, Temperature and 8 MeV electron irradiation effects on GaAs solar cells, *Pramana* 74 (2010) 995–1008.
- [24] K.A. Abdullah, F.A. Alloush, C. Salame, Investigation of the monocrystalline silicon solar cell physical behavior after thermal stress by AC impedance spectra, *Energy Proc.* 50 (2014) 30–40.
- [25] H. Asıl Üğurlu, K. Çınar Demir, C. Coşkun, The effect of thermal annealing on Ti/p-Si Schottky diodes, *J. Mater. Sci. Mater. Electron.* 32 (2021) 15343–15351.
- [26] A. Tataroğlu, F.Z. Pür, The Richardson constant and barrier inhomogeneity at Au/Si3N4/n-Si (MIS) Schottky diodes, *Phys. Scripta* 88 (2013), 015801.
- [27] M.A. Rafiq, Y. Tsuchiya, H. Mizuta, S. Oda, S. Uno, Z.A.K. Durrani, W.I. Milne, Charge injection and trapping in silicon nanocrystals, *Appl. Phys. Lett.* 87 (2005).
- [28] J.H. Joshi, D.K. Kanchan, M.J. Joshi, H.O. Jethva, K.D. Parikh, Dielectric relaxation, complex impedance and modulus spectroscopic studies of mix phase rod like cobalt sulfide nanoparticles, *Mater. Res. Bull.* 93 (2017) 63–73.
- [29] S.S. Shah, K. Hayat, S. Ali, K. Rasool, Y. Iqbal, Conduction mechanisms in lanthanum manganite nanofibers, *Mater. Sci. Semicond. Process.* 90 (2019) 65–71.